PNAS RESEARCH ARTICLE | IMMUNOLOGY AND INFLAMMATION

Differentiation and homeostasis of effector Treg cells are regulated by inositol polyphosphates modulating Ca^{2+} influx

Hyungyu Min[a], Wooseob Kim[a,1], Sehoon Hong[b], Sungkyu Lee[a], Jinguk Jeong[a], Seyun Kim[b,2], and Rho H. Seong[a,2]

Edited by Alexander Rudensky, Memorial Sloan Kettering Cancer Center, New York, NY; received November 26, 2021; accepted May 10, 2022

Activated Foxp3$^+$ regulatory T (Treg) cells differentiate into effector Treg (eTreg) cells to maintain peripheral immune homeostasis and tolerance. T cell receptor (TCR)–mediated induction and regulation of store-operated Ca^{2+} entry (SOCE) is essential for eTreg cell differentiation and function. However, SOCE regulation in Treg cells remains unclear. Here, we show that inositol polyphosphate multikinase (IPMK), which generates inositol tetrakisphosphate and inositol pentakisphosphate, is a pivotal regulator of Treg cell differentiation downstream of TCR signaling. IPMK is highly expressed in TCR-stimulated Treg cells and promotes a TCR-induced Treg cell program. IPMK-deficient Treg cells display aberrant T cell activation and impaired differentiation into RORγt$^+$ Treg cells and tissue-resident Treg cells. Mechanistically, IPMK controls the generation of higher-order inositol phosphates, thereby promoting Ca^{2+} mobilization and Treg cell effector functions. Our findings identify IPMK as a critical regulator of TCR-mediated Ca^{2+} influx and highlight the importance of IPMK in Treg cell-mediated immune homeostasis.

regulatory T cells | T cell receptor signaling | inositol polyphosphate multikinase | inositol phosphate | Ca^{2+} influx

Significance

Regulatory T (Treg) cells are indispensable for mediating self-tolerance and immune homeostasis. Treg cells expressing Foxp3 further differentiate into subtype cells residing in specific tissues. The differentiation is regulated by a process involving T cell receptor (TCR) signaling and downstream events through yet an unrevealed molecular mechanism. In this study, we show inositol polyphosphate multikinase (IPMK) as a key regulator of Treg cell differentiation. Mechanistically, IPMK-mediated production of Ins(1,3,4,5)P_4 is essential for the full activation of TCR-triggered Ca^{2+} release, providing a previously unidentified link integrating inositol polyphosphate metabolism, TCR-Ca^{2+} signaling, and Treg cell differentiation and its function. Our findings will provide a new perspective on the roles of inositol polyphosphates in Treg cell biology.

Regulatory T (Treg) cells, a subset of CD4$^+$ T cells, are indispensable for maintaining immune homeostasis and preventing autoimmune disorders (1, 2). The transcription factor forkhead box P3 (Foxp3) is essential for the development of Treg cells and for specifying their functions (2). In addition to Foxp3, Treg cells require several other factors for their transcriptional signatures and functions (3, 4). However, many such additional factors remain unknown.

Mature thymus-derived Treg (tTreg) cells migrate into peripheral tissues from the thymus and are essential for the suppression of undesired immune responses elicited by self-reactive T cells. In the periphery, CD4$^+$Foxp3$^-$ T cells can acquire Foxp3 expression and differentiate into peripherally induced Treg (pTreg) cells upon T cell receptor (TCR) stimulation under appropriate environmental cues, such as transforming growth factor beta (TGF-β) and costimulatory signals (2). Moreover, exposure to commensal bacteria and food antigens in the intestine is crucial for the generation of pTreg cells (5, 6). Additionally, tTreg cells that reside in secondary lymphoid tissues as central Treg (cTreg) cells circulate in the periphery and differentiate into effector Treg (eTreg) cells, depending on TCR stimulation. During differentiation, these cells down-regulate molecules such as CD62L and CCR7 and up-regulate CD44, chemokine receptors, and integrins to facilitate trafficking to nonlymphoid tissues (7, 8). These eTreg cells co-opt tissue-specific transcription factors, such as T-bet, Gata3, and RORγt, to acquire specialized regulatory functions, thereby being tissue-resident Treg cells that maintain immune homeostasis in parenchymal tissues (9–12).

Signal transduction through TCR plays a central role in the maintenance, differentiation, and function of Treg cells (13, 14). During TCR signaling, activated phospholipase Cγ1 generates inositol 1,4,5-trisphosphate ($InsP_3$) and diacylglycerol by hydrolyzing phosphatidylinositol 4,5-bisphosphate (15). $InsP_3$ triggers a transient increase in intracellular Ca^{2+} levels through Ca^{2+} depletion from the endoplasmic reticulum, which leads to the activation of stromal interaction molecule (STIM) and ORAI protein. This activation results in extracellular Ca^{2+} influx, called store-operated Ca^{2+} entry (SOCE), which then activates several downstream signaling effectors, including nuclear factor of activated T cells (NFAT), nuclear factor-κB (NF-κB), and other factors (16, 17).

Defects in SOCE in human patients are associated with immunodeficiency and autoimmunity, such as severe combined immunodeficiency-like disease and autoimmune hemolytic anemia (18). This emphasizes the need for SOCE in peripheral immunological tolerance. Moreover, ablation of *Stim1* and *Stim2* in mature Treg cells results in impaired SOCE, leading to reduced accumulation of tissue-resident Treg cells. This eventually results in autoantibody production and multiorgan inflammation (19). Despite the importance of

Author contributions: H.M., S.K., and R.H.S. designed research; H.M., W.K., S.H., S.L., and J.J. performed research; S.K. contributed new reagents/analytic tools; H.M., S.K., and R.H.S. analyzed data; and H.M., S.K., and R.H.S. wrote the paper.

The authors declare no competing interest.

This article is a PNAS Direct Submission.

[1]Present address: Department of Pathology and Immunology, Washington University School of Medicine in St. Louis, St. Louis, MO 63110.

[2]To whom correspondence may be addressed. Email: seyunkim@kaist.ac.kr or rhseong@snu.ac.kr.

This article contains supporting information online at http://www.pnas.org/lookup/suppl/doi:10.1073/pnas.2121520119/-/DCSupplemental.

Published July 1, 2022.

SOCE in Treg cell biology, the mechanism(s) underlying SOCE regulation is not fully understood.

Inositol polyphosphate multikinase (IPMK) is a highly conserved inositol phosphate kinase that is essential for the production of higher-order inositol phosphates. Among them, inositol tetrakisphosphate [Ins(1,3,4,5)P_4 and Ins(1,4,5,6)P_4] and inositol 1,3,4,5,6-pentakisphosphate [Ins(1,3,4,5,6)P_5] are produced by successive phosphorylation of InsP_3 through 3-kinase and 6-kinase activity of IPMK (20, 21). The importance of IPMK and higher-order inositol phosphates in immune cells has been demonstrated in a series of recent studies. InsP_6 regulates B cell receptor signaling by modulating Btk activity, thereby controlling B cell–mediated immune responses (22). Ins(1,3,4,5)P_4 is required for appropriate thymocyte development, B cell differentiation, and neutrophil function (23–25). Interestingly, a genome-wide association study of patients with inflammatory bowel disease identified four SNPs located near the *Ipmk* locus (26). Furthermore, the expression of *Ipmk* is substantially higher in colonic Treg cells than in other T cell subsets (Immunological Genome Project; ImmGen) (11). These findings suggest that IPMK is involved in the differentiation and function of Treg cells. In this study, we aimed to determine if IPMK is crucial for the SOCE-dependent transcriptional program of Treg cells and their differentiation into eTreg cells and tissue residency.

Results

IPMK Promotes Accumulation and Differentiation of Treg Cells. Treg cells reside within various parenchymal tissues, including the lung, small and large intestine, adipose tissues, skin, and secondary lymphoid tissues. These tissue-resident Treg cells regulate immune homeostasis and tissue regeneration (27–29). To investigate the physiological function of IPMK in Treg cells, we generated *Foxp3*$^{Cre\text{-}YFP}$*Ipmk*$^{fl/fl}$ mice (*Ipmk*$^{\Delta Treg}$) by crossing mice bearing loxP-flanked *Ipmk* alleles (*Ipmk*$^{fl/fl}$) with mice expressing the Foxp3-Cre recombinase/YFP fusion protein (*Ipmk*^{WT}). The ablation of *Ipmk* was confirmed by quantitative reverse transcription–polymerase chain reaction (qRT-PCR) and Western blot analysis using isolated Foxp3-YFP$^+$ Treg cells from *Ipmk*^{WT} and *Ipmk*$^{\Delta Treg}$ mice (*SI Appendix*, Fig. S1 *A* and *B*). *Ipmk*$^{\Delta Treg}$ mice displayed normal Treg cell numbers in the thymus compared with *Ipmk*^{WT} mice (*SI Appendix*, Fig. S1*C*), suggesting that deletion of IPMK in mature Treg cells does not affect the development of Treg cells in the thymus. Next, we examined the abundance of Treg cells in various tissues of *Ipmk*$^{\Delta Treg}$ mice. The frequency of Foxp3$^+$ Treg cells was significantly reduced (by ~twofold) in the large intestine lamina propria (LILP) and skin (but not in the lung) of *Ipmk*$^{\Delta Treg}$ mice compared to that in *Ipmk*^{WT} mice (Fig. 1*A*). However, the frequencies of Treg cells, including cTreg and eTreg cells, in the spleen were similar between *Ipmk*$^{\Delta Treg}$ mice and *Ipmk*^{WT} counterparts (Fig. 1 *A* and *B*). These results suggest that IPMK is required for the accumulation of tissue-resident Treg cells, particularly in the LILP and skin; however, we cannot fully exclude the possibility that reduced Treg cells in these tissues could be secondary to an increase in conventional T (Tconv) cells due to the loss of Treg cell function in the absence of IPMK.

To further examine the role of IPMK in the generation of large intestinal Treg cell subsets, we analyzed tTreg and pTreg cell populations in the LILP. We observed that RORγt$^+$ pTreg cells were markedly reduced (by ~twofold) in the LILP of *Ipmk*$^{\Delta Treg}$ mice than that of *Ipmk*^{WT} mice, whereas the frequency of Helios$^+$ tTreg cells was similar between the two mice (Fig. 1*C*). In addition, consistent with a previous report stating that RORγt$^+$ Treg cells are primary producers of interleukin (IL)-10 (12), IPMK-deficient Treg cells showed decreased expression of IL-10 than normal Treg cells did (Fig. 1*D*). This suggests the necessity of IPMK for the generation and maintenance of RORγt$^+$ pTreg cells and their regulatory functions.

Since eTreg cells co-opt specific transcription factors for their effector functions (9–12), we investigated which eTreg cell subset is regulated by IPMK. The frequency of RORγt$^+$ eTreg cells was significantly reduced in *Ipmk*$^{\Delta Treg}$ mice, particularly in the LILP. However, the frequencies of T-bet$^+$ and Gata3$^+$ eTreg cell subsets did not change significantly (Fig. 1*E*). Thus, these results support the critical role of IPMK in the differentiation and maintenance of tissue-resident Treg cells, particularly those of RORγt$^+$ Treg cells.

IPMK Is Required for Treg Cell-Mediated Suppressive Activity. Next, we examined whether IPMK deficiency affects Treg cell-mediated regulatory functions in vivo. The numbers of splenocytes and infiltrated leukocytes in the lung and LILP were slightly increased in *Ipmk*$^{\Delta Treg}$ mice than those in *Ipmk*^{WT} mice (*SI Appendix*, Fig. S2*A*). While *Ipmk*^{WT} and *Ipmk*$^{\Delta Treg}$ mice had similar frequencies of CD4$^+$ and CD8$^+$ T cells in the spleen (*SI Appendix*, Fig. S2*B*), the numbers of CD4$^+$ and CD8$^+$ T cells and the frequencies of CD62L^{lo}CD44^{hi} effector T cells were increased in the spleen and lung of *Ipmk*$^{\Delta Treg}$ mice (Fig. 2 *A* and *B* and *SI Appendix*, Fig. S2*C*). Additionally, we observed that CD4$^+$ T cells in the spleen and lung of *Ipmk*$^{\Delta Treg}$ mice produced higher levels of interferon gamma (IFN-γ) than those of *Ipmk*^{WT} mice; however, they produced similar amounts of cytokines such as IL-4, IL-13, and IL-17A. CD8$^+$ T cells in the spleen and lung of *Ipmk*$^{\Delta Treg}$ mice also produced higher levels of IFN-γ and granzyme B (GzmB) (Fig. 2*C* and *SI Appendix*, Fig. S2*D*). Furthermore, 8-mo-old *Ipmk*$^{\Delta Treg}$ mice displayed weight loss (*SI Appendix*, Fig. S2*E*) and elevated immune cell infiltration in various nonlymphoid tissues compared to that in age-matched *Ipmk*^{WT} mice (*SI Appendix*, Fig. S2*F*). Although the abundance of Treg cells appeared normal in the spleen and lung of *Ipmk*$^{\Delta Treg}$ mice, these observations suggest that IPMK ablation in Treg cells contributes to their functional defects.

To directly evaluate the requirement for IPMK in Treg cell-mediated suppressive activity, we conducted an in vivo suppression assay. When *Rag2*$^{-/-}$ mice were adoptively transferred to induce colitis with CD45.1$^+$CD4$^+$CD45RB^{hi} congenic naive T cells alone or with Treg cells isolated from the *Ipmk*$^{\Delta Treg}$ and *Ipmk*^{WT} mice, the IPMK-deficient Treg cells showed markedly reduced suppressive capacity, as indicated by the progressive body weight loss, increased intestinal pathology, higher frequency of IFN-γ–producing CD4$^+$ T cells (Fig. 2 *D*–*F*), shortening of colon length, and reduced ratio of Treg cells to Tconv cells in recipient mice (*SI Appendix*, Fig. S2 *G* and *H*).

The functional consequences of IPMK deficiency in Treg cells were further investigated using a dextran sodium sulfate (DSS)-induced acute intestinal inflammation model (30), in which Treg cells control inflammation in an IL-10–dependent manner (31). *Ipmk*$^{\Delta Treg}$ mice displayed exacerbated weight loss, colon shortening, and colon tissue destruction (*SI Appendix*, Fig. S3 *A*–*C*), indicating impaired protection due to defective Treg cell function. Flow cytometric analysis revealed that the overall cellularity of LILP, T cells, and neutrophils was increased (*SI Appendix*, Fig. S3*D*). In contrast, the frequency of Treg cells in LILP was reduced, and IL-10 expression in Treg cells was impaired in *Ipmk*$^{\Delta Treg}$ mice (*SI Appendix*, Fig. S3 *E* and *F*). Collectively, these data further support that IPMK is essential for Treg cell-mediated immunosuppression in peripheral tissues.

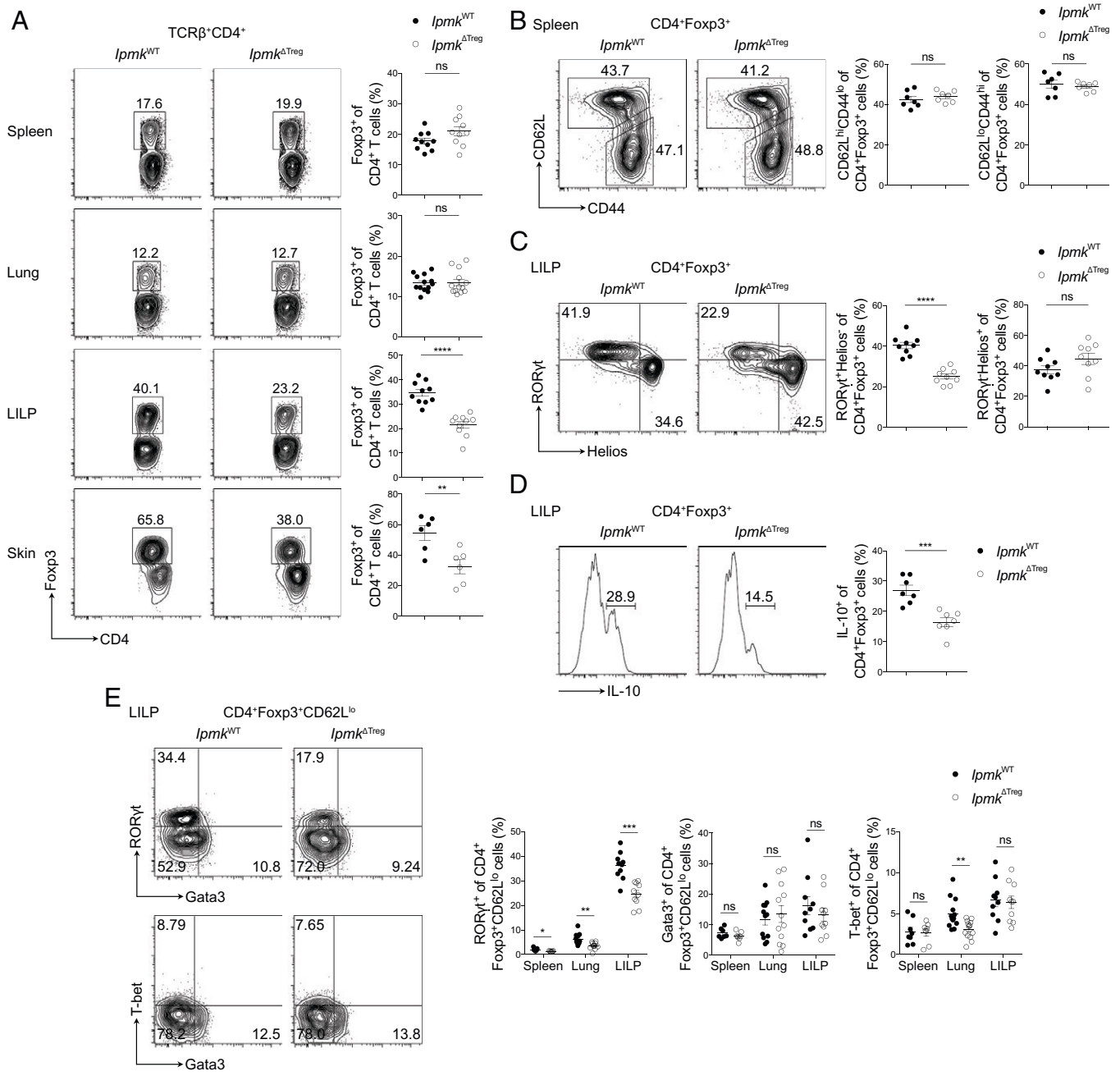

Fig. 1. Treg cells require IPMK for their differentiation and accumulation in nonlymphoid tissues. (*A*) Flow cytometry analysis of Foxp3 in CD4$^+$ T cells in the spleen, lung, LILP, and skin of *Ipmk*^{WT} and *Ipmk*$^{\Delta Treg}$ mice. Graphs show percentages of CD4$^+$Foxp3$^+$ Treg cells (n = 6–13). (*B*) Flow cytometry analysis of CD62L and CD44 in CD4$^+$Foxp3$^+$ Treg cells isolated from the spleen of *Ipmk*^{WT} and *Ipmk*$^{\Delta Treg}$ mice. Graphs show percentages of CD62L^{hi}CD44^{lo} cTreg cells and CD62L^{lo}CD44^{hi} eTreg cells among CD4$^+$Foxp3$^+$ Treg cells (n = 7). (*C*) Flow cytometry analysis of RORγt and Helios in CD4$^+$Foxp3$^+$ Treg cells isolated from the LILP of *Ipmk*^{WT} and *Ipmk*$^{\Delta Treg}$ mice. Graphs show percentages of RORγt$^+$ Treg cells and Helios$^+$ Treg cells among CD4$^+$Foxp3$^+$ Treg cells in LILP (n = 9). (*D*) Flow cytometry analysis of intracellular IL-10 in CD4$^+$Foxp3$^+$ Treg cells isolated from the LILP of *Ipmk*^{WT} and *Ipmk*$^{\Delta Treg}$ mice and stimulated with phorbol myristate acetate (PMA, 50 ng/mL) and ionomycin (500 ng/mL) for 4 h. The graph shows percentages of IL-10-producing cells among CD4$^+$Foxp3$^+$ Treg cells (n = 7). (*E*) Flow cytometry analysis of expression of RORγt, Gata3, and T-bet in CD4$^+$Foxp3$^+$CD62L^{lo} Treg cells isolated from the LILP of *Ipmk*^{WT} and *Ipmk*$^{\Delta Treg}$ mice. Graphs show percentages of cells expressing RORγt, Gata3, and T-bet among CD4$^+$Foxp3$^+$CD62L^{lo} Treg cells from indicated organs (n = 7–13). Multiple unpaired t tests with Holm-Sidak multiple comparison correction were used for statistical analyses (*E*). Otherwise, unpaired Student's t test was used for statistical analyses. Error bars represent the mean ± SEM values. ns, not significant; *P < 0.05; **P < 0.01; ***P < 0.001; ****P < 0.0001.

Treg Cells Require IPMK to Inhibit Anti-Tumor Immune Responses. Treg cells are recruited and accumulated in various tumor tissues and suppress effector T cell–mediated immune responses against tumor-associated antigens (32, 33). Thus, we examined whether targeting IPMK activity in Treg cells increases T cell–mediated anti-tumor immunity. When we inoculated B16-F10 melanoma cells, tumor growth was significantly inhibited in *Ipmk*$^{\Delta Treg}$ mice compared to that in *Ipmk*^{WT} mice (Fig. 3*A*). Flow cytometric analysis of tumor-infiltrating lymphocytes (TILs) revealed that the numbers of both CD4$^+$ and CD8$^+$ T cells were increased (Fig. 3*B*), and the ratio of CD4$^+$ to CD8$^+$ T cells was reduced in *Ipmk*$^{\Delta Treg}$ mice (Fig. 3*C*). In addition, the frequency of tumor-infiltrating Treg cells was markedly reduced in *Ipmk*$^{\Delta Treg}$ mice (Fig. 3*D*), which was accompanied by an increased ratio of CD4$^+$ or CD8$^+$ T cells to Treg cells (Fig. 3*E*), supporting the augmented anti-tumor immune responses. Furthermore, IPMK ablation in Treg cells resulted in enhanced IFN-γ and GzmB

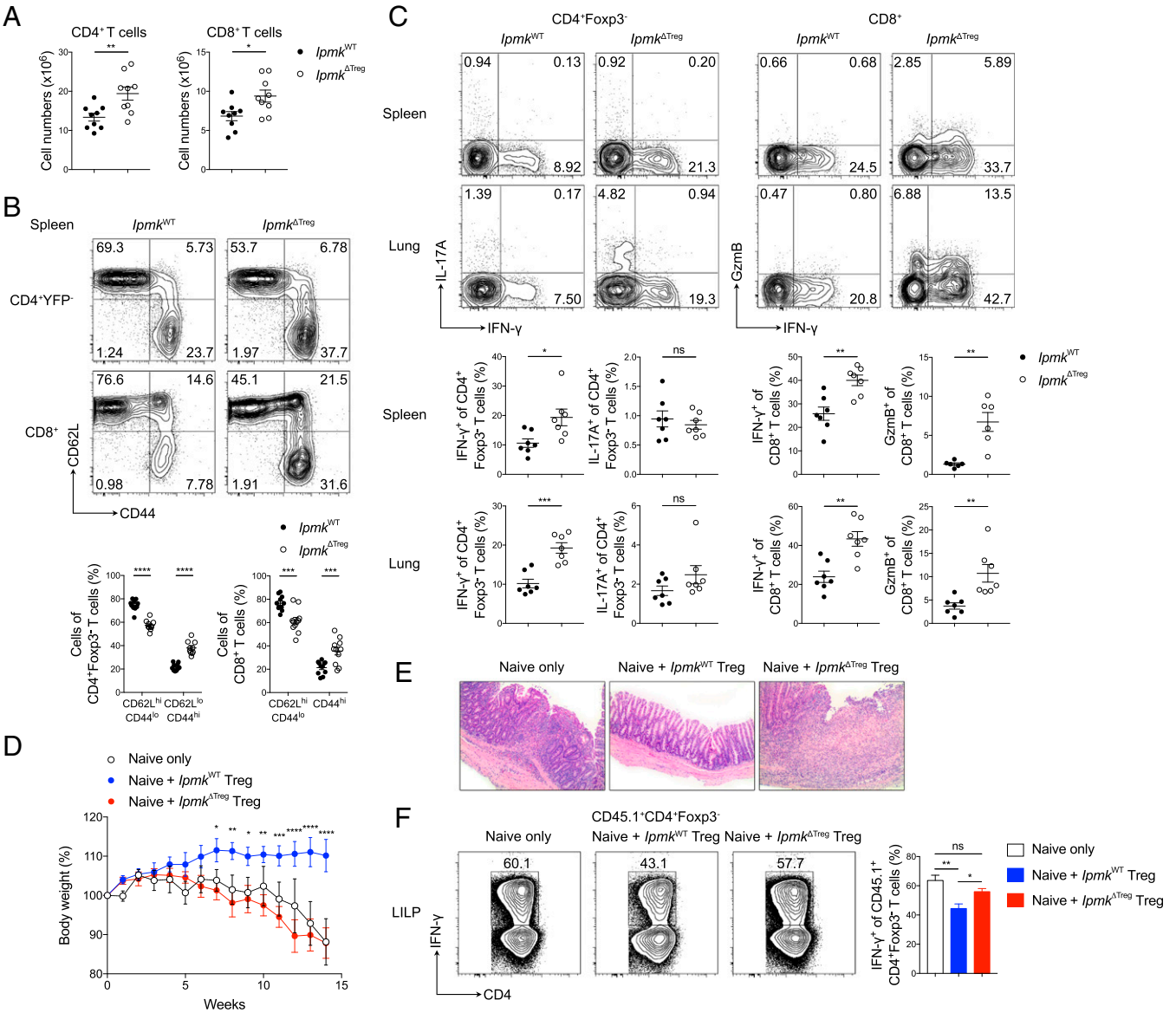

Fig. 2. IPMK-deficient Treg cells show impaired suppressive function. (*A*) Graphs show numbers of CD4$^+$ and CD8$^+$ T cells in the spleen of *Ipmk*^{WT} and *Ipmk*$^{\Delta Treg}$ mice (n = 10–12). (*B*) Flow cytometry analysis of CD62L and CD44 in CD4$^+$Foxp3$^-$ and CD8$^+$ T cells isolated from the spleen of *Ipmk*^{WT} and *Ipmk*$^{\Delta Treg}$ mice. Graphs show percentages of CD62L^{hi}CD44^{lo} naive cells and CD62L^{lo}CD44^{hi} activated cells among CD4$^+$Foxp3$^-$ and CD8$^+$ T cells (n = 10–11). (*C*) Flow cytometry analysis of intracellular IFN-γ and IL-17A in CD4$^+$Foxp3$^-$ T cells and IFN-γ and granzyme B (GzmB) in CD8$^+$ T cells isolated from the spleen and lung of *Ipmk*^{WT} and *Ipmk*$^{\Delta Treg}$ mice and stimulated with PMA (50 ng/mL) and ionomycin (500 ng/mL) for 4 h. Graphs show percentages of CD4$^+$ and CD8$^+$ T cells producing the indicated cytokines (n = 6–7). (*D–F*) In vivo suppression assay using CD4$^+$Foxp3-YFP$^+$ Treg cells purified from *Ipmk*^{WT} and *Ipmk*$^{\Delta Treg}$ mice. Sex-matched *Rag2*$^{-/-}$ mice were transferred with CD4$^+$CD25$^-$CD45RB^{hi} naive T cells alone or with CD4$^+$Foxp3-YFP$^+$ Treg cells. (*D*) The graph shows body weight changes during in vivo suppression assay (n = 4–7). (*E*) Hematoxylin and eosin staining of the colon from *Rag2*$^{-/-}$ recipients in each group. (*F*) Flow cytometry analysis of intracellular IFN-γ in CD45.1$^+$CD4$^+$ T cells purified from the LILP in each group and cultured for 4 h in the presence of PMA (50 ng/mL) and ionomycin (500 ng/mL). The graph shows percentages of IFN-γ$^+$CD4$^+$ T cells among CD45.1$^+$ T cells (n = 4–5). Two-way ANOVA (*D*) or one-way ANOVA (*F*) with Tukey's multiple comparison test was used for statistical analyses. Otherwise, unpaired Student's t test was used for statistical analyses. Error bars represent the mean ± SEM values. ns, not significant; *P < 0.05; **P < 0.01; ***P < 0.001; ****P < 0.0001.

expression in CD4$^+$ and CD8$^+$ T cells, respectively (Fig. 3*F*). These findings indicate that IPMK modulates the regulatory activity of Treg cells to inhibit anti-tumor immune responses; therefore, targeting IPMK in Treg cells would be an innovative approach for improving tumor therapy.

IPMK Is Indispensable for eTreg Cell Generation and Homeostasis. We have shown that IPMK is essential for the differentiation and function of Treg cells. To examine the Treg cell-intrinsic properties of IPMK under noninflammatory conditions, we employed two approaches. First, we generated mixed bone marrow (BM) chimeric mice by reconstituting BM-depleted *Rag2*$^{-/-}$ mice with BM cells from CD45.1$^+$ wild-type (WT) mice with BM cells from CD45.2$^+$ *Ipmk*^{WT} or *Ipmk*$^{\Delta Treg}$ mice (Fig. 4*A*). Second, we generated *Foxp3*$^{Cre/Thy1.1}$ *Ipmk*$^{fl/fl}$ female mice having both IPMK-deficient Treg cells (Cre-expressing cells) and IPMK-sufficient Treg cells (Thy1.1-expressing cells). These mice still contain WT Treg cells and thus, are protected from tissue inflammation. In both situations, the ratio of IPMK-deficient Treg cells to IPMK-sufficient Treg cells in the spleen was reduced, and this was more obvious in the BM and nonlymphoid tissues (Fig. 4 *B* and *C*), suggesting that IPMK regulates the competitive fitness of Treg cells and accumulation of tissue-resident Treg cells in a cell-intrinsic manner.

Consistent with the finding that the absence of IPMK led to preferential reduction of Treg cells in nonlymphoid tissues

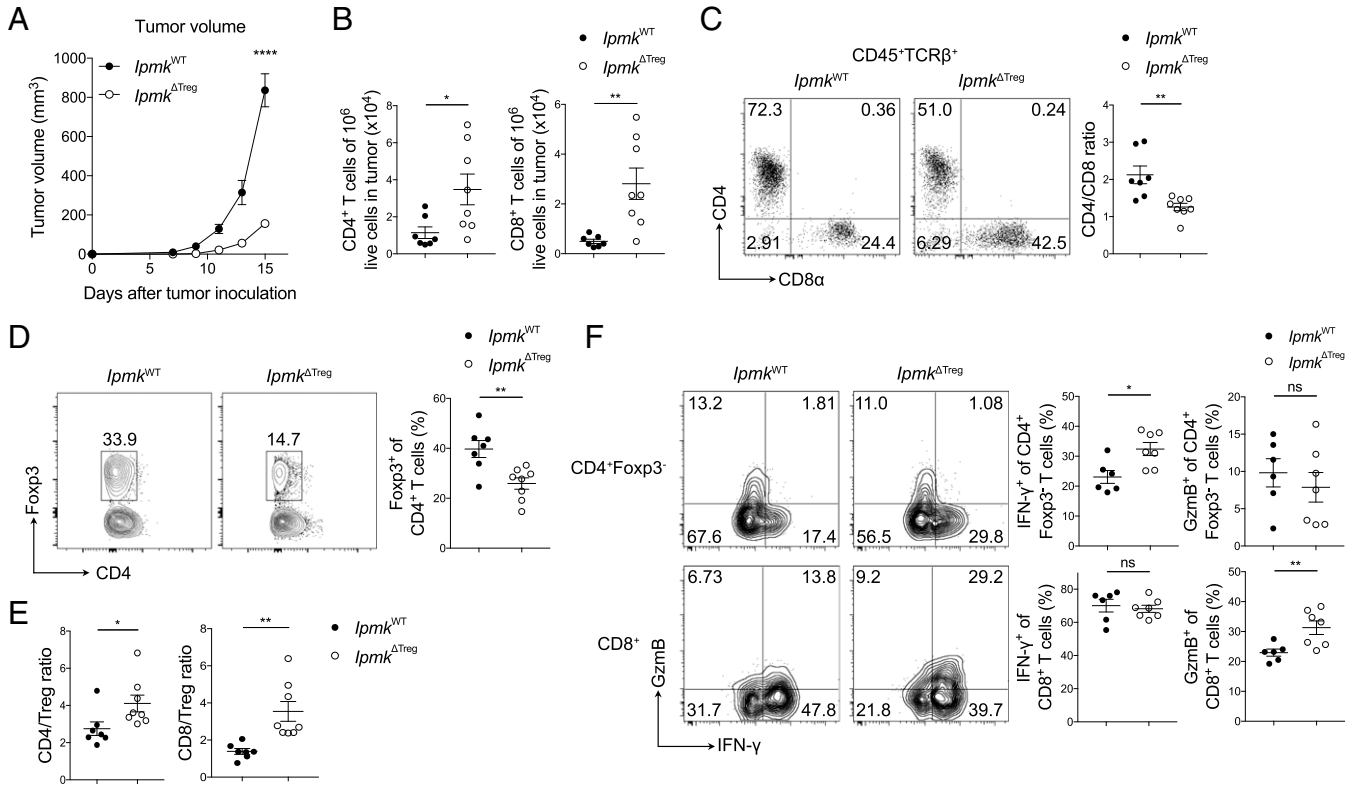

Fig. 3. Treg cell-specific ablation of IPMK results in enhanced anti-tumor immunity. *Ipmk*^{WT} and *Ipmk*$^{\Delta Treg}$ mice were inoculated subcutaneously with B16F10 melanoma cells. (*A*) The graph shows tumor growth during tumor progression, expressed as mean tumor volume (mm^3) (n = 7–10). (*B*) Graphs show numbers of CD4$^+$ and CD8$^+$ T cells among 10^6 live cells in TILs (n = 7–8). (*C*) Flow cytometry analysis of CD4 and CD8 in TCRβ$^+$ cells isolated from the tumor of *Ipmk*^{WT} and *Ipmk*$^{\Delta Treg}$ mice. The graph shows ratios of CD4$^+$ to CD8$^+$ T cells among TCRβ$^+$ T cells in TILs (n = 7–8). (*D*) Flow cytometry analysis of Foxp3 in TCRβ$^+$CD4$^+$ T cells isolated from the tumor of *Ipmk*^{WT} and *Ipmk*$^{\Delta Treg}$ mice. The graph shows percentages of Foxp3$^+$ Treg cells among CD4$^+$ T cells in TILs (n = 7–8). (*E*) Graphs show ratios of CD4$^+$ to CD4$^+$Foxp3$^+$ Treg cells and CD8$^+$ to CD4$^+$Foxp3$^+$ Treg cells among TCRβ$^+$ T cells in TILs (n = 7–8). (*F*) Flow cytometry analysis of intracellular IFN-γ and GzmB in CD4$^+$ and CD8$^+$ T cells in the tumor of *Ipmk*^{WT} and *Ipmk*$^{\Delta Treg}$ mice after cultured for 4 h in the presence of PMA (50 ng/mL) and ionomycin (500 ng/mL). Graphs show percentages of IFN-γ$^+$ and GzmB$^+$ CD4$^+$ T cells and IFN-γ$^+$ and GzmB$^+$ CD8$^+$ T cells among TCRβ$^+$ T cells in TILs (n = 6–7). Two-way ANOVA was used for statistical analysis in (*A*). Otherwise, unpaired Student's t test was used for statistical analyses. Error bars represent the mean ± SEM values. ns, not significant; *P < 0.05; **P < 0.01; ****P < 0.0001.

such as LILP and the skin, which consist mainly of eTreg cells (Figs. 1*A* and 4 *B* and *C*), IPMK-deficient Treg cells, in *Foxp3*$^{Cre/Thy1.1}$*Ipmk*$^{fl/fl}$ mice, displayed a significant reduction in CD62L^{lo}CD44^{hi} Treg cells than in IPMK-sufficient Treg cells (Fig. 4*D* and *SI Appendix*, Fig. S4*A*). This reduction of eTreg cells was more pronounced in the BM, LILP, and skin (*SI Appendix*, Fig. S4*B*). This was also represented by the decreased expression of ICOS, PD-1, CTLA4, and GITR, which are typically expressed in eTreg cells (7) (Fig. 4*E* and *SI Appendix*, Fig. S4*C*). Since differentiation of cTreg cells into eTreg cells is accompanied by cell proliferation (7), we assessed the proliferation capacity of Treg cells and found that IPMK-deficient Treg cells expressed Ki-67 at a reduced level (Fig. 4*F*). These results suggest that IPMK intrinsically promotes eTreg cell differentiation.

To further establish the importance of IPMK in eTreg cell differentiation, we performed activation-induced eTreg cell differentiation experiments. When CD62L^{hi}CD44^{lo} cTreg cells isolated from the *Ipmk*$^{\Delta Treg}$ and *Ipmk*^{WT} mice were activated in vitro, the differentiation of IPMK-deficient cTreg cells into CD62L^{lo}CD44^{hi} eTreg-like cells was less efficient (Fig. 4*G*). In addition, the differentiation of IPMK-deficient Treg cells into RORγt$^+$ Treg cells was inefficient when cells were cultured in the presence of IL-6 and IL-23 (Fig. 4*H*) (34). Collectively, these results suggest that IPMK is essential for eTreg and tissue-resident Treg cell differentiation.

IPMK Globally Regulates the Transcriptional Program of Treg Cells. When the transcriptional profiles of CD4$^+$YFP$^+$Thy1.1$^-$ Treg cells isolated from *Foxp3*$^{Cre/Thy1.1}$ and *Foxp3*$^{Cre/Thy1.1}$*Ipmk*$^{fl/fl}$ female mice were analyzed (Fig. 5*A*), 432 genes were differentially expressed between the groups; 279 genes were down-regulated and 153 genes were up-regulated in IPMK-deficient cells (>1.5-fold, P value <0.05) (Fig. 5*B*). Gene set enrichment analysis (GSEA) revealed that common Treg signature genes (35) were underrepresented in IPMK-deficient Treg cells (Fig. 5*C*). The expression of transcription factors such as *Ahr*, *Batf*, *Maf*, and *Prdm1*, which facilitate Treg cell differentiation and function, was down-regulated in the IPMK-deficient Treg cells, whereas *Tcf7* and *Satb1*, mostly associated with the naive state, were up-regulated. In addition, the IPMK-deficient Treg cells displayed reduced expression of genes for cell surface molecules indicative of activated or eTreg cells (e.g., *Lag3*, *Icos*, *Il1rl1*, *Pdcd1*, and *Klrg1*), regulatory molecules associated with immune suppression (e.g., *Gzmb*, *Nt5e*, *Fgl2*, and *Il18*), and integrins and chemokine receptors that control the migration of Treg cells (Fig. 5*D*).

GSEA with hallmark gene sets from the MSigDB (36) revealed that the IL-2/STAT5 signaling pathway was suppressed in IPMK-deficient cells (Fig. 5*E*). Furthermore, gene sets associated with fatty acid metabolism and E2F targets related to the active cell cycle and target genes of the NF-κB signaling pathway were underrepresented in IPMK-deficient cells (Fig. 5 *F* and *G* and *SI Appendix*, Fig. S5). By qRT-PCR,

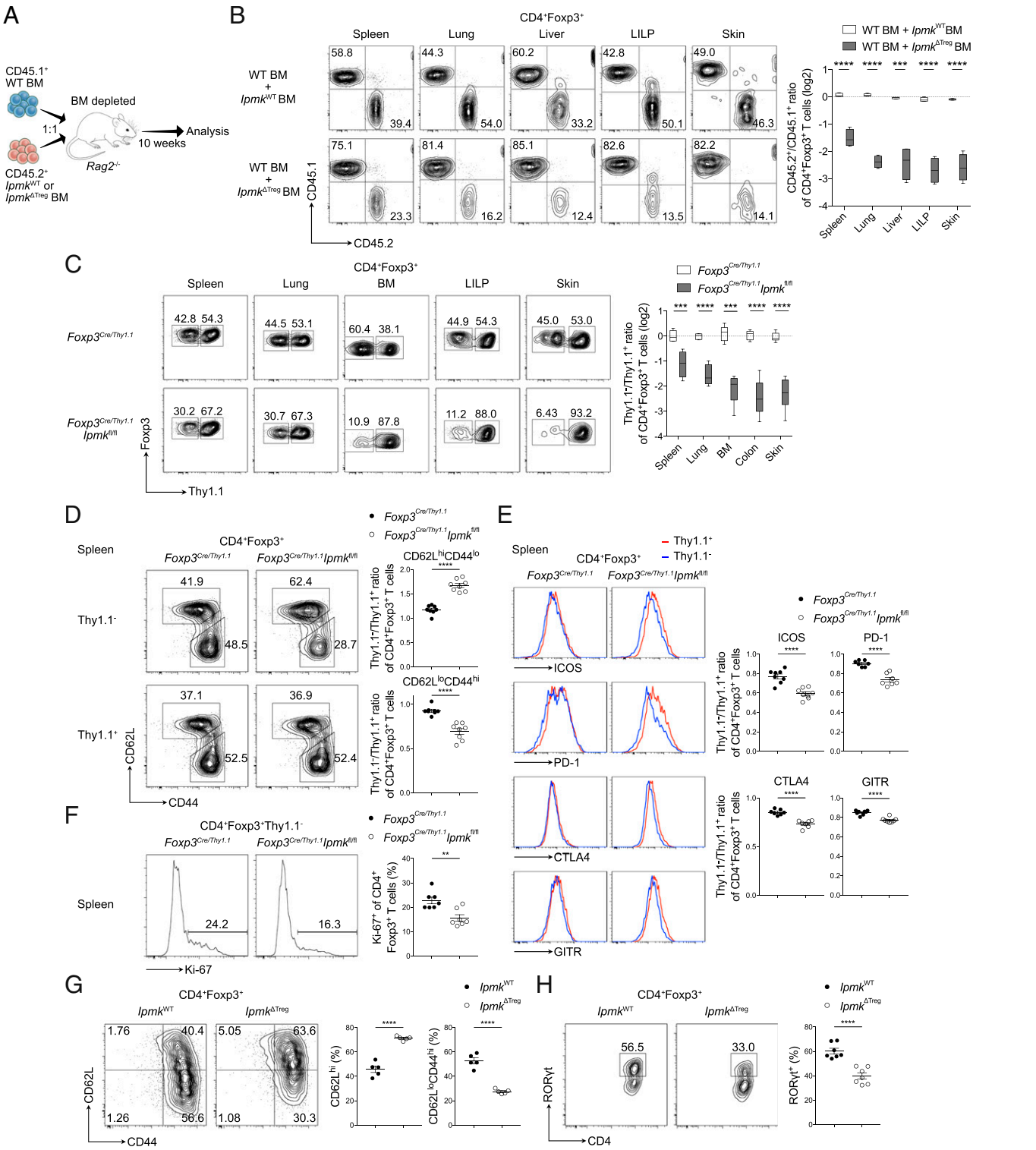

Fig. 4. IPMK controls eTreg cell generation and homeostasis in a cell-intrinsic manner. (*A*) Schematic representation of the generation of mixed bone marrow (BM) chimeric mice. (*B*) Flow cytometry analysis of CD45.1 and CD45.2 in $CD4^+Foxp3^+$ Treg cells isolated from the spleen, lung, liver, LILP, and skin of mixed BM chimeric mice. The graph shows ratios of $CD45.2^+$ to $CD45.1^+$ cells among $CD4^+Foxp3^+$ Treg cells from indicated organs ($n = 4$). (*C*) Flow cytometry analysis of Thy1.1 in $CD4^+Foxp3^+$ Treg cells isolated from the spleen, lung, BM, LILP, and skin of *Foxp3*$^{Cre/Thy1.1}$ and *Foxp3*$^{Cre/Thy1.1}$*Ipmk*$^{fl/fl}$ mice. The graph shows ratios of $Thy1.1^-$ to $Thy1.1^+$ cells among $CD4^+Foxp3^+$ Treg cells from indicated organs ($n = 5$–8). (*D*) Flow cytometry analysis of CD62L and CD44 in $CD4^+Foxp3^+Thy1.1^-$ and $CD4^+Foxp3^+Thy1.1^+$ Treg cells isolated from the spleen of *Foxp3*$^{Cre/Thy1.1}$ and *Foxp3*$^{Cre/Thy1.1}$*Ipmk*$^{fl/fl}$ mice. Graphs show ratios of $Thy1.1^-$ to $Thy1.1^+$ cells in $CD62L^{hi}CD44^{lo}$ cTreg cells and $CD62L^{lo}CD44^{hi}$ eTreg cells among $CD4^+Foxp3^+$ Treg cells ($n = 8$). (*E*) Flow cytometry analysis of ICOS, PD-1, CTLA4, and GITR in $CD4^+Foxp3^+Thy1.1^-$ and $CD4^+Foxp3^+Thy1.1^+$ Treg cells isolated from the spleen of *Foxp3*$^{Cre/Thy1.1}$ and *Foxp3*$^{Cre/Thy1.1}$*Ipmk*$^{fl/fl}$ mice. Graphs show ratios of MFI of indicated molecules in $Thy1.1^-$ cells to that in $Thy1.1^+$ cells among $CD4^+Foxp3^+$ Treg cells ($n = 7$–8). (*F*) Flow cytometry analysis of Ki-67 in $CD4^+Foxp3^+Thy1.1^-$ Treg cells isolated from the spleen of *Foxp3*$^{Cre/Thy1.1}$ and *Foxp3*$^{Cre/Thy1.1}$*Ipmk*$^{fl/fl}$ mice. The graph shows percentages of $Ki\text{-}67^+$ Treg cells among $CD4^+Foxp3^+$ Treg cells ($n = 7$–8). (*G*) Flow cytometry analysis of CD62L and CD44 in cTreg cells purified from spleen of *Ipmk*^{WT} and *Ipmk*$^{\Delta Treg}$ mice and stimulated with anti-CD3/CD28 and IL-2 for 3 d. Graphs show percentages of $CD62L^{hi}$ Treg cells and $CD62L^{lo}CD44^{hi}$ Treg cells ($n = 5$). (*H*) Flow cytometry analysis of RORγt expression in Treg cells purified from spleen of *Ipmk*^{WT} and *Ipmk*$^{\Delta Treg}$ mice and stimulated with anti-CD3/CD28 in the presence of IL-2, IL-6, and IL-23 for 3 d. The graph shows percentages of $ROR\gamma t^+$ Treg cells ($n = 7$). Unpaired Student's *t* test was used for statistical analyses. Error bars represent the mean ± SEM values. $^{**}P < 0.01$; $^{***}P < 0.001$; $^{****}P < 0.0001$.

we further validated the expression of representative genes in control and IPMK-deficient Treg cells (Fig. 5*H*). This pattern of deregulated gene sets in the absence of IPMK is similar to that of Treg cells defective in Ca^{2+} signaling (19). Therefore, these results suggest that IPMK might function via the TCR-induced Ca^{2+} signaling pathway in Treg cells.

IPMK Is Required for TCR-Induced Ca^{2+} Mobilization in Treg Cells. IPMK is highly expressed in Treg cells isolated from nonlymphoid tissues, especially the LILP and skin, compared to those isolated from lymphoid tissues such as the spleen and mesenteric lymph nodes (mLN) (Fig. 6*A*). The intestine and skin are continuously exposed to antigenic challenges, such as commensal microorganisms and nutrients; this provides a consistent stimulation of TCR in Treg cells. Consistent with this notion, the expression of activation markers, such as CD69 and CD44, and eTreg cell markers including CD103, GITR, and KLRG1 (28) was highly elevated in Treg cells from nonlymphoid tissues, particularly in the LILP and skin, compared to those in the spleen (Fig. 6*B* and *SI Appendix*, Fig. S6). TCR stimulation of splenic Treg cells resulted in a substantial increase in *Ipmk* mRNA expression (Fig. 6*C*). Moreover, it induces the expression of *Irf4* and *c-myc* via activation of the NF-κB pathway (37–39) and the immunosuppressive cytokine-encoding gene *Il10* (40). However, IPMK-deficient Treg cells displayed reduced mRNA expression of *Irf4*, *c-myc*, and *Il10* upon TCR stimulation (Fig. 6 *D* and *E*), strongly suggesting that IPMK regulates TCR signaling and the expression of downstream target genes in Treg cells.

High-performance liquid chromatography revealed reduced higher-order InsPs, such as $InsP_5$, $InsP_6$, and $InsP_7$ in the extract of IPMK-deficient Treg cells (Fig. 6*F*). Synthesis of $InsP_4$ was also significantly reduced in these cells, even though the process is mediated by both ITPKB and IPMK. IPMK generates both types of $InsP_4$, $Ins(1,3,4,5)P_4$ and $Ins(1,4,5,6)P_4$, from $InsP_3$. $Ins(1,3,4,5)P_4$, unlike $Ins(1,4,5,6)P_4$, has been shown to hinder $InsP_3$ 5-phosphatase-mediated $InsP_3$ metabolism, thereby facilitating receptor-mediated Ca^{2+} mobilization by sensitizing $InsP_3$-mediated Ca^{2+} influx (41). Consistent with this finding, IPMK-deficient Treg cells indeed exhibited reduced $InsP_3$ levels compared to that in control Treg cells (Fig. 6*F*). When Ca^{2+}-sensitive dye-loaded $CD4^+CD25^+$ T cells, which are mostly $Foxp3^+$ Treg cells (Fig. 6*G*), were stimulated with anti-CD3, SOCE was noticeably impaired in IPMK-deficient $CD4^+CD25^+$ T cells (Fig. 6*H*). Reduced SOCE could have resulted from the TCR-independent pathway or direct regulation of CRAC channel machinery expression by IPMK. However, treatment of $CD4^+CD25^+$ T cells with thapsigargin, which activates SOCE in a TCR-independent manner, resulted in a similar level of SOCE between IPMK-deficient and control cells (Fig. 6*I*). The expression of STIM1 and STIM2 proteins (i.e., critical regulators of CRAC channel activation) was not altered in IPMK-deficient cells (*SI Appendix*, Fig. S7). In addition, cell-permeable $Ins(1,3,4,5)P_4$ supplementation during stimulation of IPMK-deficient cells restored the impaired Ca^{2+} response (Fig. 6*J*). However, the enantiomer $Ins(1,4,5,6)P_4$ failed to rescue the Ca^{2+} response of IPMK-deficient cells (Fig. 6*K*). Furthermore, when IPMK-deficient Treg cells were treated with calcium ionophore, defects in TCR-mediated gene expression were restored (Fig. 6 *L* and *M*), further confirming that they were Ca^{2+}-dependent. These results suggest that IPMK regulates Ca^{2+} mobilization in a TCR- and $Ins(1,3,4,5)P_4$-dependent manner without directly altering the expression of the CRAC channel machinery. Thus, we argue that IPMK is crucial in Treg cells for proper TCR signal transduction and effector outcomes via the regulation of intracellular $Ins(1,3,4,5)P_4$.

Discussion

Our results show that IPMK is essential for the regulatory function and differentiation of Treg cells into eTreg subsets and their accumulation in nonlymphoid tissues and that IPMK fine-tunes Treg cell function and identity, which are maintained by TCR-dependent Ca^{2+} influx.

We observed that ablation of IPMK in Treg cells resulted in the reduction of Treg cells in a context-dependent manner. The accumulation of Treg cells was similar in the spleen and lung of $Ipmk^{WT}$ and $Ipmk^{\Delta Treg}$ mice. However, the accumulation of IPMK-deficient Treg cells was significantly impaired in the presence of WT Treg cells. In addition, tissue-resident Treg cells in the LILP and skin, mostly eTreg cells, were significantly reduced in $Ipmk^{\Delta Treg}$ mice, which was further enhanced in competitive environments, suggesting that IPMK might control the competitive fitness of Treg cells in addition to their differentiation capacity. Given that Treg and Tconv cells utilize the same homeostatic mediators such as costimulatory molecules and cytokines for their proliferation and differentiation, there appears to be a competition between eTreg and effector Tconv cells, in addition to that among Treg cells (42). The notion that IPMK-deficient eTreg cells possess an impaired ability to compete with effector Tconv cells might partly explain the inflammatory phenotype in the spleen of $Ipmk^{\Delta Treg}$ mice despite the normal eTreg cell frequency among splenic Treg cells. Although observed elsewhere (34, 43, 44), it is not clear why defective Treg cells accumulate normally in lymphoid tissues under inflammatory conditions despite the reduced tissue-resident Treg cells. Nevertheless, our results support that IPMK is essential for maintaining Treg cell homeostasis in a competitive environment.

IPMK-deficient Treg cells displayed impaired Ca^{2+} influx and accumulation of tissue-resident Treg cells. It has been shown that mature Treg cell-specific abolishment of SOCE hinders the differentiation of Treg cells into tissue-resident Treg cells and their effector functions, whereas the number of tTreg cells remains unaltered (19). Our results show that IPMK positively regulates the expression of genes associated with eTreg cell identity (e.g., *Ahr*, *Prdm1*, *Batf*, and *Maf*), function (e.g., *Gzmb* and *Nt5e*), and localization (e.g., *Itgae*, *Itgb8*, *Ccr2*, and *Ccr10*), which are also regulated by SOCE (19). In addition, our GSEA results showed that the IL-2/STAT5 signaling pathway and fatty acid metabolism were deregulated in the absence of IPMK. IL-2 signaling is required for proliferation and function of Treg cells by controlling fatty acid oxidation (FAO), on which Treg cells are generally dependent for their metabolic requirements (45). The fact that intracellular Ca^{2+} links TCR and IL-2 signaling with FAO suggests that IPMK might orchestrate the transcriptional network, at least in part, by regulating TCR-mediated Ca^{2+} signaling.

Ca^{2+} signals regulate the activity of NF-κB in T cells (46), implying that IPMK might function as a regulator of NF-κB in Treg cells by controlling Ca^{2+} signaling. In addition to impaired TCR-induced expression of *Irf4* and *c-myc*, multiple genes that were down-regulated in Treg cells with defective NF-κB signaling (e.g., *Prdm1*, *Batf*, *Il1rl1*, *Icos*, *Tigit*, *Klrg1*, *Nt5e*, and *Gzmb*) (34, 47, 48) were also down-regulated in IPMK-deficient Treg cells. p65 might have a key role in the differentiation of eTreg cells in competitive environments (47). Treg cell-specific ablation of c-Rel confers enhanced anti-tumor

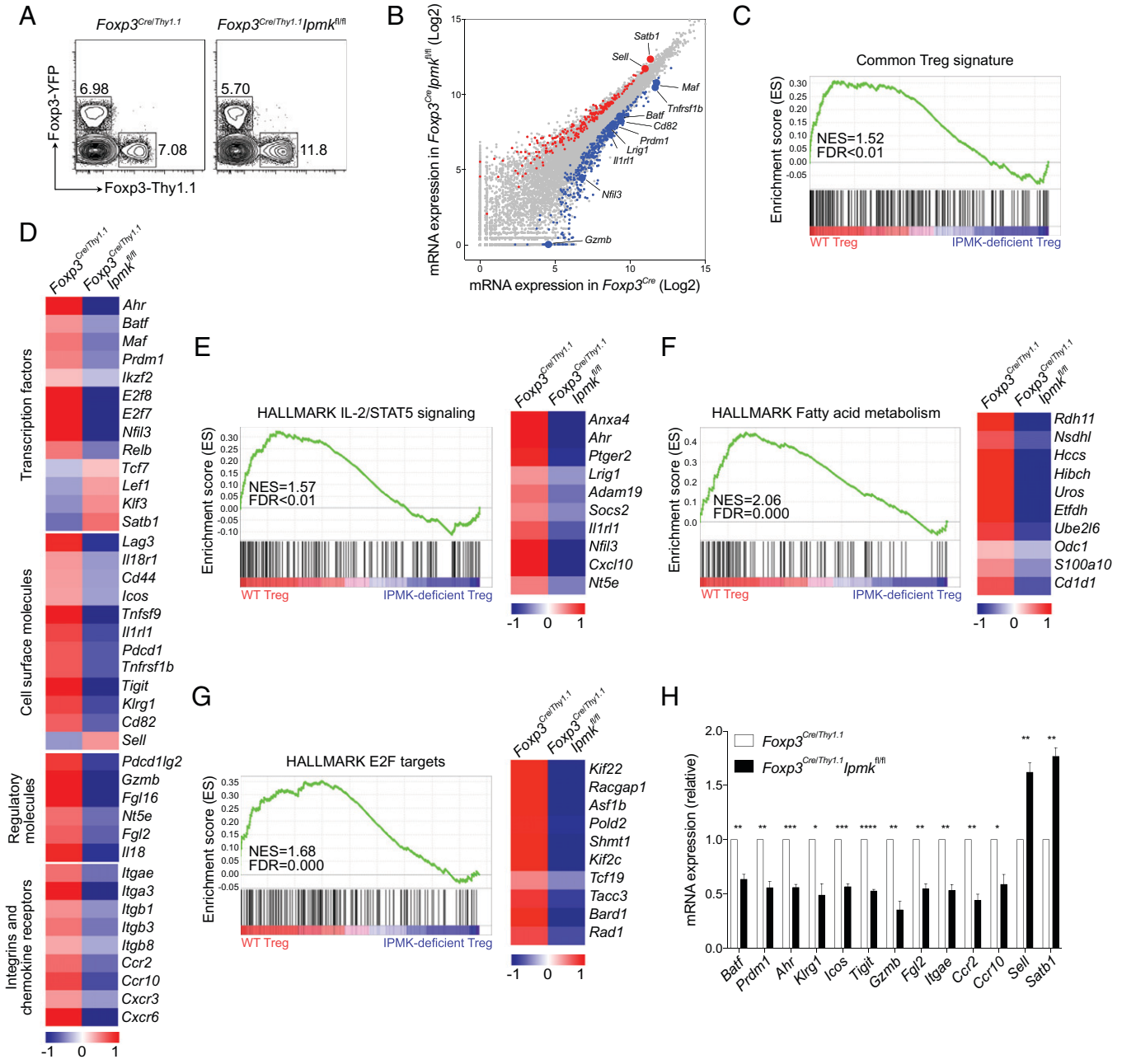

Fig. 5. IPMK regulates transcriptional networks in Treg cells. RNA-sequencing analysis of CD4$^+$YFP$^+$ Treg cells isolated from the spleen of *Foxp3*$^{Cre/Thy1.1}$ and *Foxp3*$^{Cre/Thy1.1}$*Ipmk*$^{fl/fl}$ mice. (*A*) Flow cytometry analysis of expression of YFP and Thy1.1 in CD4$^+$ T cells isolated from the spleen of *Foxp3*$^{Cre/Thy1.1}$ and *Foxp3*$^{Cre/Thy1.1}$*Ipmk*$^{fl/fl}$ mice. (*B*) Gene expression profile of YFP$^+$ Treg cells isolated from *Foxp3*$^{Cre/Thy1.1}$*Ipmk*$^{fl/fl}$ mice versus those from *Foxp3*$^{Cre/Thy1.1}$ mice. (*C*) Gene set enrichment analysis (GSEA) comparing the relative expression of common Treg signature genes in WT versus IPMK-deficient Treg cells. (*D*) Heatmap analysis of Treg cell-related genes expression in WT versus IPMK-deficient Treg cells, shown in groups based on their function. (*E–G*) GSEA comparing the relative expression of genes involved in IL-2/STAT5 signaling (*E*), fatty acid metabolism (*F*), and that of E2F target genes (*G*). (*H*) Validation of gene expression changes in control and IPMK-deficient Treg cells using quantitative RT-PCR ($n = 3$). Multiple unpaired *t* tests with Holm-Sidak multiple comparison correction were used for statistical analysis. Error bars represent the mean ± SEM values. **P* < 0.05; ***P* < 0.01; ****P* < 0.001; *****P* < 0.0001.

immune responses, resulting from their impaired regulatory activity against CD8$^+$ T cells (48). In line with these results, IPMK-deficient mice showed impaired Treg cell infiltration in the tumor microenvironment that resulted in augmented T cell–mediated anti-tumor responses, thereby reducing the growth of implanted melanoma. This phenotypic similarity exhibited by the defects in NF-κB and IPMK signaling is further supported by the underrepresentation of NF-κB target genes in IPMK-deficient Treg cells, as determined by GSEA. Thus, specific inhibition of IPMK activity in Treg cells could be an effective therapeutic strategy for cancer immunotherapy.

IPMK generates $InsP_4$ and $InsP_5$ through sequential phosphorylation of $InsP_3$. Although these inositol-derived metabolites are produced in large amounts upon TCR stimulation, their physiological functions as second messengers have not been revealed, particularly in Treg cells. Among these higher-order InsPs, $Ins(1,3,4,5)P_4$ has recently been identified as a regulator of the development and function of T cells, B cells, and neutrophils (23, 24, 49). In this study, we showed that IPMK-deficient Treg cells display reduced production of $InsP_4$ and subsequent reduction in $InsP_3$ along with defects in Ca^{2+} mobilization. This defect was restored by exogenous $Ins(1,3,4,5)P_4$, suggesting that IPMK is essential for $Ins(1,3,4,5)P_4$-mediated regulation of TCR-

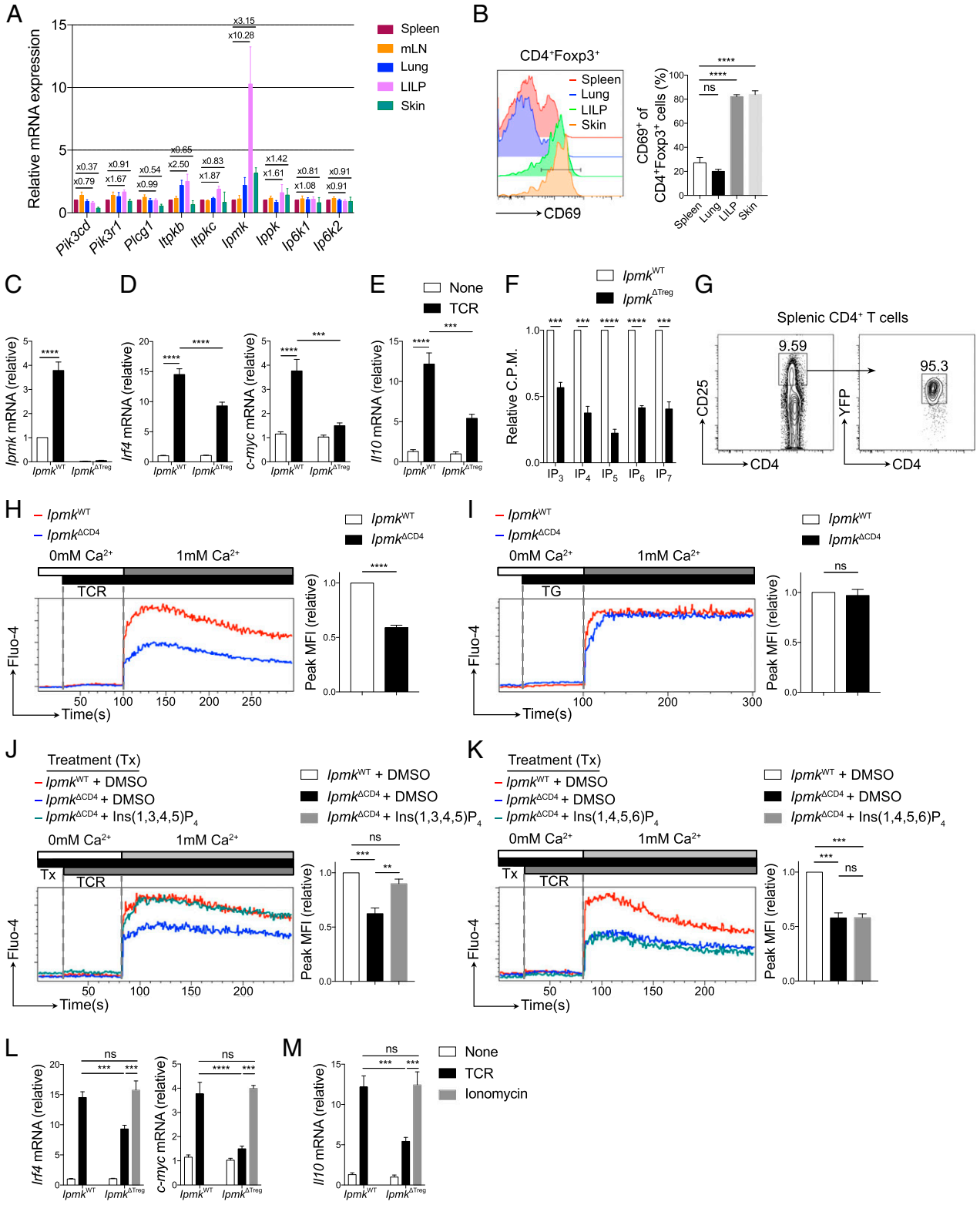

Fig. 6. IPMK controls TCR-induced SOCE by regulating the production of Ins(1,3,4,5)P_4 in Treg cells. (*A*) Quantitative RT-PCR analysis of indicated genes in Treg cells isolated from the spleen, mLN, lung, LILP, and skin ($n = 3$). (*B*) Flow cytometry analysis of CD69 expression in Treg cells in the spleen, lung, LILP, and skin. The graph shows percentages of $CD69^+$ Treg cells among $CD4^+Foxp3^+$ Treg cells ($n = 4$). (*C–E*) Quantitative RT-PCR analysis of *Ipmk* (*C*), *Irf4*, *c-myc* (*D*), and *Il10* (*E*) in Treg cells activated with anti-CD3 and anti-CD28 for 4 h ($n = 4–6$). (*F*) The graph shows the relative counts per minute (C.P.M.) of soluble InsPs extracted from Treg cells radiolabeled with [^{3}H]myo-inositol in the presence of anti-CD3 and anti-CD28 ($n = 3$). (*G*) Flow cytometry analysis of Foxp3-YFP expression in $CD4^+CD25^+$ T cells isolated from the spleen. (*H–K*) Analysis of Ca^{2+} influx with the Ca^{2+}-sensitive dye Fluo-4 NW. (*H* and *I*) Analysis of Ca^{2+} influx in $CD4^+CD25^+$ T cells stimulated with anti-CD3 (*H*) or thapsigargin (TG) (*I*) in the absence of exogenous Ca^{2+}, followed by the addition of 1 mM Ca^{2+}. The graphs show the relative MFI of peaks of Ca^{2+} influx ($n = 6–8$). (*J* and *K*) Analysis of Ca^{2+} influx in $CD4^+CD25^+$ T cells after the addition of cell-permeable Ins(1,3,4,5)P_4 (5 μM) (*J*) or Ins(1,4,5,6)P_4 (5 μM) (*K*), then anti-CD3, followed by the addition of 1 mM Ca^{2+}. The graphs show the relative MFI of peaks of Ca^{2+} influx ($n = 3–4$). (*L* and *M*) Quantitative RT-PCR analysis of *Irf4*, *c-myc* (*L*), and *Il10* (*M*) in Treg cells activated with anti-CD3 and anti-CD28 for 4 h in the absence or presence of calcium ionophore (50 ng/mL) ($n = 3–4$). One-way ANOVA with the Tukey's multiple comparison test was used for statistical analyses (*B–E*, *J* and *K*). Otherwise, unpaired Student's *t* test was used for statistical analyses. Error bars represent the mean ± SEM values. ns, not significant; $^{**}P < 0.01$; $^{***}P < 0.001$; $^{****}P < 0.0001$.

induced SOCE in Treg cells. This is further supported by the results that thapsigargin-stimulated Treg cells, in which $InsP_3$ is barely produced, show unaltered SOCE activity in the absence of IPMK.

$InsP_3$ is converted to $Ins(1,3,4,5)P_4$ by $InsP_3$ 3-kinases, such as ITPKA, ITPKB, ITPKC, and IPMK. Among these, ITPKB and IPMK are abundant and have an essential function in the immune system (22–24). Previous reports showed that ITPKB regulates thymocyte development by controlling the production of $Ins(1,3,4,5)P_4$ (23); thus, it is possible that ITPKB might mask the function of IPMK in Treg cells, which is not the case. Interestingly, the expression patterns of IPMK and ITPKB are different in thymocytes and Treg cells. Public RNA-sequencing data (ImmGen) show that ITPKB is highly expressed in DP thymocytes, suggesting its exclusive function for $Ins(1,3,4,5)P_4$ production in thymocytes. Our expression analysis of inositol phosphates- and phosphoinositide-metabolizing enzymes in Treg cells from various tissues revealed that IPMK was markedly expressed in tissue-resident Treg cells than in Treg cells from lymphoid tissues, whereas no substantial changes were observed in the expression of the other $InsP_3$ 3-kinases (Fig. 6*A*). Thus, it is very likely that IPMK critically regulates the differentiation of eTreg and tissue-resident Treg cells as a major regulator of $Ins(1,3,4,5)P_4$ in Treg cells.

In summary, we identified IPMK as a key regulator of the transcriptional program, differentiation, regulatory function, and competitive ability of eTreg and tissue-resident Treg cells. IPMK finely modulates $Ins(1,3,4,5)P_4$ production and thereby regulates $InsP_3$-mediated SOCE in Treg cells. Therefore, these features of inositol polyphosphates tunable by IPMK in Treg cells may offer therapeutic strategies for curing autoimmune diseases, allergies, and cancer.

Materials and Methods

Mice. Strategy for the generation of *Ipmk*$^{fl/fl}$ mice was previously described (50). *Foxp3*$^{IRES\text{-}YFP\text{-}Cre}$ and *Foxp3*$^{Thy1.1}$ mice were kindly provided by Alexander Rudensky. *Rag2*$^{-/-}$ (stock #008449), B6SJL (stock #002014), and *Cd4*^{Cre} (stock #017336) mice were purchased from The Jackson Laboratory. All animals were maintained on a C57BL/6 background and bred in specific pathogen-free barrier facilities at Seoul National University and Institute of Molecular Biology and Genetics, and were used in accordance with protocols approved by the Institutional Animal Care and Use Committees of Seoul National University.

A detailed description of all materials and methods is available in *SI Appendix, SI Materials and Methods*.

Data Availability. All study data are included in the article and/or *SI Appendix*.

ACKNOWLEDGMENTS We thank our laboratory members for helpful advice and discussions. This work was supported in part by the National Research Foundation of Korea (NRF-2021R1A2B5B03002202 to R.H.S. and NRF-2018R1A5A1024261 and NRF-2020R1A2C3005765 to S.K.), Korea Mouse Phenotyping Project (NRF-2014M3A9D5A01073789 to R.H.S.) of the Ministry of Science, Information and Communication Technology, and Future Planning through the National Research Foundation.

Author affiliations: [a]School of Biological Sciences and Institute of Molecular Biology and Genetics, Seoul National University, Seoul 08826, Korea; and [b]Department of Biological Sciences, Korea Advanced Institute of Science and Technology, Daejeon 34141, Korea

1. S. Sakaguchi, T. Yamaguchi, T. Nomura, M. Ono, Regulatory T cells and immune tolerance. *Cell* **133**, 775–787 (2008).
2. S. Z. Josefowicz, L. F. Lu, A. Y. Rudensky, Regulatory T cells: Mechanisms of differentiation and function. *Annu. Rev. Immunol.* **30**, 531–564 (2012).
3. M. Feuerer, J. A. Hill, D. Mathis, C. Benoist, Foxp3+ regulatory T cells: Differentiation, specification, subphenotypes. *Nat. Immunol.* **10**, 689–695 (2009).
4. M. A. Gavin *et al.*, Foxp3-dependent programme of regulatory T-cell differentiation. *Nature* **445**, 771–775 (2007).
5. J. L. Round, S. K. Mazmanian, Inducible Foxp3+ regulatory T-cell development by a commensal bacterium of the intestinal microbiota. *Proc. Natl. Acad. Sci. U.S.A.* **107**, 12204–12209 (2010).
6. S. K. Lathrop *et al.*, Peripheral education of the immune system by colonic commensal microbiota. *Nature* **478**, 250–254 (2011).
7. K. S. Smigiel *et al.*, CCR7 provides localized access to IL-2 and defines homeostatically distinct regulatory T cell subsets. *J. Exp. Med.* **211**, 121–136 (2014).
8. M. D. Rosenblum, S. S. Way, A. K. Abbas, Regulatory T cell memory. *Nat. Rev. Immunol.* **16**, 90–101 (2016).
9. A. G. Levine *et al.*, Stability and function of regulatory T cells expressing the transcription factor T-bet. *Nature* **546**, 421–425 (2017).
10. E. A. Wohlfert *et al.*, GATA3 controls Foxp3$^+$ regulatory T cell fate during inflammation in mice. *J. Clin. Invest.* **121**, 4503–4515 (2011).
11. E. Sefik *et al.*, MUCOSAL IMMUNOLOGY. Individual intestinal symbionts induce a distinct population of RORγ$^+$ regulatory T cells. *Science* **349**, 993–997 (2015).
12. C. Ohnmacht *et al.*, MUCOSAL IMMUNOLOGY. The microbiota regulates type 2 immunity through RORγt$^+$ T cells. *Science* **349**, 989–993 (2015).
13. A. G. Levine, A. Arvey, W. Jin, A. Y. Rudensky, Continuous requirement for the TCR in regulatory T cell function. *Nat. Immunol.* **15**, 1070–1078 (2014).
14. J. C. Vahl *et al.*, Continuous T cell receptor signals maintain a functional regulatory T cell pool. *Immunity* **41**, 722–736 (2014).
15. X. C. Liao, D. R. Littman, Altered T cell receptor signaling and disrupted T cell development in mice lacking Itk. *Immunity* **3**, 757–769 (1995).
16. S. Feske, Calcium signalling in lymphocyte activation and disease. *Nat. Rev. Immunol.* **7**, 690–702 (2007).
17. M. O. Li, A. Y. Rudensky, T cell receptor signalling in the control of regulatory T cell differentiation and function. *Nat. Rev. Immunol.* **16**, 220–233 (2016).
18. R. S. Lacruz, S. Feske, Diseases caused by mutations in ORAI1 and STIM1. *Ann. N. Y. Acad. Sci.* **1356**, 45–79 (2015).
19. M. Vaeth *et al.*, Tissue resident and follicular Treg cell differentiation is regulated by CRAC channels. *Nat. Commun.* **10**, 1183 (2019).
20. A. Saiardi, H. Erdjument-Bromage, A. M. Snowman, P. Tempst, S. H. Snyder, Synthesis of diphosphoinositol pentakisphosphate by a newly identified family of higher inositol polyphosphate kinases. *Curr. Biol.* **9**, 1323–1326 (1999).
21. J. P. Frederick *et al.*, An essential role for an inositol polyphosphate multikinase, Ipk2, in mouse embryogenesis and second messenger production. *Proc. Natl. Acad. Sci. U.S.A.* **102**, 8454–8459 (2005).
22. W. Kim *et al.*, Inositol polyphosphates promote T cell-independent humoral immunity via the regulation of Bruton's tyrosine kinase. *Proc. Natl. Acad. Sci. U.S.A.* **116**, 12952–12957 (2019).
23. V. Pouillon *et al.*, Inositol 1,3,4,5-tetrakisphosphate is essential for T lymphocyte development. *Nat. Immunol.* **4**, 1136–1143 (2003).
24. A. T. Miller *et al.*, Production of Ins(1,3,4,5)P4 mediated by the kinase Itpkb inhibits store-operated calcium channels and regulates B cell selection and activation. *Nat. Immunol.* **8**, 514–521 (2007).
25. K. Sauer, M. P. Cooke, Regulation of immune cell development through soluble inositol-1,3,4,5-tetrakisphosphate. *Nat. Rev. Immunol.* **10**, 257–271 (2010).
26. J. S. Yokoyama *et al.*; Alzheimer's Disease Neuroimaging Initiative, Association between genetic traits for immune-mediated diseases and Alzheimer disease. *JAMA Neurol.* **73**, 691–697 (2016).
27. D. Cipolletta *et al.*, PPAR-γ is a major driver of the accumulation and phenotype of adipose tissue Treg cells. *Nature* **486**, 549–553 (2012).
28. N. Arpaia *et al.*, A distinct function of regulatory T cells in tissue protection. *Cell* **162**, 1078–1089 (2015).
29. N. Ali *et al.*, Regulatory T cells in skin facilitate epithelial stem cell differentiation. *Cell* **169**, 1119–1129.e11 (2017).
30. B. Chassaing, J. D. Aitken, M. Malleshappa, M. Vijay-Kumar, Dextran sulfate sodium (DSS)-induced colitis in mice. *Curr. Protoc. Immunol.* **104**, 15.25.11–15.25.14 (2014).
31. T. Jofra *et al.*, Experimental colitis in IL-10-deficient mice ameliorates in the absence of PTPN22. *Clin. Exp. Immunol.* **197**, 263–275 (2019).
32. W. Zou, Regulatory T cells, tumour immunity and immunotherapy. *Nat. Rev. Immunol.* **6**, 295–307 (2006).
33. H. Nishikawa, S. Sakaguchi, Regulatory T cells in tumor immunity. *Int. J. Cancer* **127**, 759–767 (2010).
34. A. Vasanthakumar *et al.*, The TNF receptor superfamily-NF-κB axis is critical to maintain effector regulatory T cells in lymphoid and non-lymphoid tissues. *Cell Rep.* **20**, 2906–2920 (2017).
35. J. A. Hill *et al.*, Foxp3 transcription-factor-dependent and -independent regulation of the regulatory T cell transcriptional signature. *Immunity* **27**, 786–800 (2007).
36. A. Liberzon *et al.*, The molecular signatures database (MSigDB) hallmark gene set collection. *Cell Syst.* **1**, 417–425 (2015).
37. K. Man *et al.*, The transcription factor IRF4 is essential for TCR affinity-mediated metabolic programming and clonal expansion of T cells. *Nat. Immunol.* **14**, 1155–1165 (2013).
38. R. Nayar *et al.*, TCR signaling via Tec kinase ITK and interferon regulatory factor 4 (IRF4) regulates CD8+ T-cell differentiation. *Proc. Natl. Acad. Sci. U.S.A.* **109**, E2794–E2802 (2012).
39. R. Wang *et al.*, The transcription factor Myc controls metabolic reprogramming upon T lymphocyte activation. *Immunity* **35**, 871–882 (2011).
40. A. Scheffold, J. Hühn, T. Höfer, Regulation of CD4+CD25+ regulatory T cell activity: It takes (IL-)two to tango. *Eur. J. Immunol.* **35**, 1336–1341 (2005).
41. M. C. Hermosura *et al.*, InsP4 facilitates store-operated calcium influx by inhibition of InsP3 5-phosphatase. *Nature* **408**, 735–740 (2000).
42. A. Liston, D. H. Gray, Homeostatic control of regulatory T cell diversity. *Nat. Rev. Immunol.* **14**, 154–165 (2014).
43. N. Hayatsu *et al.*, Analyses of a mutant Foxp3 allele reveal BATF as a critical transcription factor in the differentiation and accumulation of tissue regulatory T cells. *Immunity* **47**, 268–283.e9 (2017).

44. S. I. Koizumi *et al.*, JunB regulates homeostasis and suppressive functions of effector regulatory T cells. *Nat. Commun.* **9**, 5344 (2018).
45. M. Y. Fan, L. A. Turka, Immunometabolism and PI(3)K signaling as a link between IL-2, Foxp3 expression, and suppressor function in regulatory T cells. *Front. Immunol.* **9**, 69 (2018).
46. L. Palkowitsch *et al.*, The Ca2+-dependent phosphatase calcineurin controls the formation of the Carma1-Bcl10-Malt1 complex during T cell receptor-induced NF-kappaB activation. *J. Biol. Chem.* **286**, 7522–7534 (2011).
47. N. Messina *et al.*, The NF-κB transcription factor RelA is required for the tolerogenic function of Foxp3(+) regulatory T cells. *J. Autoimmun.* **70**, 52–62 (2016).
48. Y. Grinberg-Bleyer *et al.*, NF-κB c-Rel is crucial for the regulatory T cell immune checkpoint in cancer. *Cell* **170**, 1096–1108.e13 (2017).
49. Y. Jia *et al.*, Inositol trisphosphate 3-kinase B (InsP3KB) as a physiological modulator of myelopoiesis. *Proc. Natl. Acad. Sci. U.S.A.* **105**, 4739–4744 (2008).
50. S. Kim *et al.*, Amino acid signaling to mTOR mediated by inositol polyphosphate multikinase. *Cell Metab.* **13**, 215–221 (2011).